VIBRATION-BASED DAMAGE DETECTION IN A BEAM STRUCTURE WITH MULTIPLE DAMAGE LOCATIONS

Sandris Rucevskis [1], Miroslaw Wesolowski [2], Andris Chate [3]

Institute of Materials and Structures, Riga Technical University, Azenes St. 16-323, LV-1048, Riga, Latvia
E-mails: [1] sandris_r@bf.rtu.lv; [2] mwesolowski@c4.bf.rtu.lv; [3] and_cate@latnet.lv

Sandris RUCEVSKIS, M.Sc
Date of birth: March 20, 1979.
Education: 2003 - Masters Degree in civil engineering, Riga Technical University.
Experience: Researcher, Institute of Materials and Structures, Riga Technical University
Fields of research: mechanics of composite materials, dynamics of structures, damage detection, numerical methods and computer analysis of structures.

Miroslaw WESOLOWSKI, M.Sc
Date of birth: February 26, 1981.
Education: 2006 - Masters Degree in mechanical engineering, Military University of Technology in Warsaw.
Experience: Researcher, Institute of Materials and Structures, Riga Technical University
Fields of research: strength and dynamics of structures, damping analysis, mechanics of solid and composite materials, numerical methods and computer analysis of structures.

Andris CHATE, Prof., Dr.Sc.ing
Date of birth: July 5, 1952
Education: 1981 - PhD in mechanical engineering, Riga Technical University.
Experience: Professor, Institute of Materials and Structures, Riga Technical University.
Publications: Author of more than 140 different scientific publications.
Fields of research: strength and dynamics of structures, damping analysis, mechanics of composite materials, numerical methods and computer analysis of structures, fracture mechanics.

Abstract

During the last two decades structural damage identification using dynamic parameters of the structure has become an important research area for civil, mechanical, and aerospace engineering communities. The basic idea of the vibration-based damage detection methods is that a damage as a combination of different failure modes in the form of loss of local stiffness in the structure alters its dynamic characteristics, i.e., the modal frequencies, mode shapes, and modal damping values. A great variety of methods have been proposed for damage detection by using dynamic structure parameters; however, most of them require modal data of the healthy state of structure as a reference. In this paper a vibration-based damage detection method which uses the mode shape information determined from only the damaged state of the structure is proposed. To establish the method, two aluminium beams containing different sizes of mill-cut damage at a single location as well as two aluminium beams containing different sizes of mill-cut damage at multiple locations are examined. The experimental modal frequencies and the corresponding mode shapes for the first 15 flexural modes are obtained by using a scanning laser vibrometer with a PZT actuator. From the mode shapes, mode shape curvatures are obtained by using a central difference approximation. In order to exclude the influence of measurement noise on the modal data and misleading damage indices, it is proposed to use the sum of mode shape curvature squares for each mode. With the example of the beams with free-free and clamped boundary conditions, it is shown that the mode shape curvature squares can be used to detect damage in the structures. The extent of mill-cut damage is identified via the modal frequencies by using mixed numerical-experimental technique. The method is based on the minimization of the discrepancy between the numerically calculated and the experimentally measured frequencies. The numerical frequencies are calculated by employing a finite-element model for beam with introduced damage. Further, by using the response surface approach, a relationship (second-order polynomial function) between the modal frequencies and the damage extent is constructed. The damage extent is obtained by solving the minimization problem.

Keywords: Damage detection, dynamic response, mode shape curvature, scanning laser vibrometer.

1. Introduction

Many structural applications worldwide have been in use for tens or even hundreds of years. Their failure could lead to tragic consequences and therefore structures have regular costly inspections. The standard procedure of performing routine maintenance and replacing parts before they have actually used up their life is inefficient and increases the cost of the structure. For example currently 27% of an average aircraft's life cycle cost is spent on inspection and repair [1]. The strong need to develop effective damage identification techniques for structural health monitoring and damage detection at the earliest possible stage is pervasive throughout the civil, mechanical, and aerospace engineering industries. Damage identification can increase safety,

extend serviceability, reduce maintenance costs and define reducing operating limits for structures.
During the last decades vibration-based damage detection methods have attracted the most attention due to their simplicity for implementation. These methods are based on the fact that the dynamic characteristics, i.e., the natural frequencies, mode shapes, and modal damping are directly related to the stiffness of the structure. Therefore, a change in natural frequencies or a change in mode shapes will indicate a loss of the stiffness. Valuable reviews of the state of art in the methods for detecting, localizing, and characterizing damage by examining the changes in the measured vibration parameters can be found in [2,3]. Many studies have investigated the effects of damage on mode shapes [4-6] and corresponding mode shape curvatures [7-9]. These papers show that mode shape curvatures are highly sensitive to damage and can be used to localize it. However, the major drawback of those methods is a need for the data of the healthy structure which sometimes could be difficult to obtain or even impossible. To overcome this issue Gapped Smoothing Techniques [10-12] were introduced which allow the damage detection in a structure without prior knowledge on the healthy state. The basic idea of the methods is that the mode shape curvature of the healthy structure has a smooth surface, and it can be approximated by a polynomial. The square of the difference between the measured curvature and the smoothed polynomial is defined as damage index and maximum value indicates the location and size of the damage.
In the present paper the method which uses the mode shape curvature squares determined from only the damaged state of the structure for the damage detection in a beam is described and compared with other relevant damage detection methods referenced in literature. The experimental modal frequencies and the corresponding mode shapes obtained by using a scanning laser vibrometer with a PZT actuator are used for illustration of the proposed method. In addition damage extent is identified via the modal frequencies by using a mixed numerical-experimental technique.

2. Damage detection algorithms

Since the mode shape curvature squares are derived from mode shapes and also for a better illustration of the proposed method, it was decided to compare the present method with other relevant damage detection methods which employ mode shape information.

2.1 Mode shape (MS) damage index

The simplest one is the mode shape damage index. It represents the difference between the mode shapes of the healthy and the damaged structures [4]

$$\Delta v_i = \left| v_i^d - v_i \right| \tag{1}$$

where v^d_i and v_i are mode shapes of the damaged and the healthy state of a structure, respectively, and i denotes the node number or measured point.
The experimentally measured mode shapes are inevitably corrupted by measurement noise. This noise introduces local perturbations to the mode shape which can lead to peaks in the mode shape slope, curvature and curvature square profiles. These peaks could be mistakenly interpreted as damage or they could mask the peaks induced by real damage in a beam and lead to false or missed detection of damage. To overcome this problem, it is proposed to average the sum of damage indices from each mode. To summarize the results for all modes, the index is proposed as

$$MS = \frac{1}{N}\sum_{n=1}^{N}\left(\Delta v_i\right)_n \tag{2}$$

where N is the total number of modes to be considered.

2.2 Mode shape slope (MSS) damage index

This algorithm uses the change in the mode shape slope

$$\Delta v_i^{'} = \left| v_i^{'d} - v_i^{'} \right| \tag{3}$$

The central difference approximation is used to derive the mode shape slope from the mode shape

$$v_i^{'} = \frac{\left(v_{i+1} - v_{i-1}\right)}{2h} \tag{4}$$

where h is the distance between two successive nodes or measured points.
If more than one mode is used, the index is given by

$$MSS = \frac{1}{N}\sum_{n=1}^{N}\left(\Delta v_i^{'}\right)_n \tag{5}$$

2.3 Mode shape curvature (MSC) damage index

In this algorithm the location of damage is assessed by the difference in the mode shape curvature between the healthy and the damaged case [7]

$$\Delta v_i^{''} = \left| v_i^{''d} - v_i^{''} \right| \tag{6}$$

The mode shape curvatures is computed from experimentally measured or numerically calculated mode shapes using the central difference approximation

$$v_i^{''} = \frac{\left(v_{i+1} - 2v_i + v_{i-1}\right)}{h^2} \tag{7}$$

The sum of the damage indices from each mode is defined by

$$MSC = \frac{1}{N}\sum_{n=1}^{N}\left(\Delta v_i''\right)_n \quad (8)$$

2.4 Mode shape curvature square (MSCS) damage index

This damage index is defined by [4]

$$\Delta v_i''^2 = \left| v_i''^{d2} - v_i''^2 \right| \quad (9)$$

For more than one mode used, the index is

$$MSCS = \frac{1}{N}\sum_{n=1}^{N}\left(\Delta v_i''^2\right)_n \quad (10)$$

All the aforementioned methods assess the location of the damage by the largest computed absolute difference between the mode shape function of the damaged and the healthy state of a structure. However, the major drawback of those methods is a need for the data of the healthy structure which sometimes could be difficult to obtain or even impossible. To overcome this issue it was proposed to use the mode shape curvature squares from only the damaged state of the beam as a damage index.

2.5 Mode shape curvature square magnitude (MSCSM) damage index

The vibration strain energy (U_i) associated with the particular mode shape at a point is given by

$$U_i = \frac{1}{2}\int_x EI\left(v_i''\right)^2 dx \quad (11)$$

where v_i'' is the mode shape curvature and EI is the flexural stiffness of the structure. The idea of the proposed method is based on the relationship between the mode shape curvature square and the flexural stiffness of a structure. Damage induced reduction of the flexural stiffness of the structure subsequently causes an increase in the magnitude of the mode shape curvature square. The increase of the magnitude of the curvature square is local in nature, thus the mode shape curvature square may be considered as an indicator for the damage location. The location of the damage is assessed by the largest magnitude of the mode shape curvature square. The summarized damage index for all modes is proposed as

$$MSCSM = \frac{1}{N}\sum_{n=1}^{N}\left(v_i''^2\right)_n \quad (12)$$

3. Case study 1 – aluminium beams with a single damage location

In order to establish the proposed damage detection method two aluminium beams containing single mill-cut damage at different locations have been examined.

3.1 Geometry of the beams and numerical analysis

To verify the validity and effectiveness of the damage algorithms introduced above, the numerical modal analysis based on the finite element (FE) method was performed. The numerical analysis was carried out by using the commercial FE software ANSYS. Geometrical configuration of the beams is shown in Figure 1. Dimensions of the *Beam 1* are as follows: length L = 1250 mm, width B = 50 mm and thickness H = 5 mm. Mill-cut damage with depth of 2 mm and size of 50 mm is introduced at a distance of 750 mm from one edge of the beam. The *Beam 2* dimensions are 1500 x 50 x 5 mm. Damage with depth of 2 mm and size of 100 mm is introduced at a distance of 950 mm.

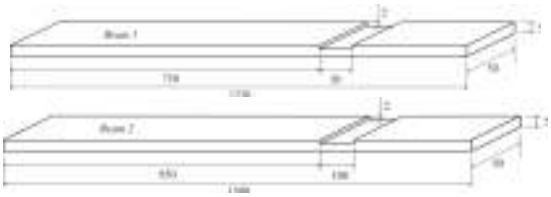

Fig. 1. Geometry and dimensions of the test beams containing mill-cut damage at single location.

Experimentally determined material properties are: Young's modulus E = 69 GPa, Poission ratio ν = 0.31 and mass density ρ = 2708 kg/m3. Finite element models for beams consist of two dimensional beam elements (ANSYS 11.0). Each node has three degrees of freedom, namely translations along the X and Y axes and rotation along the Z axis. Finite element length of 10 mm is considered, thus the *Beam 1* is constructed by means of 125 equal length elements (i=126 nodes) and the *Beam 2* -150 elements (i=151 nodes). For the healthy beam, a constant stiffness EI is assumed for all elements, while the damaged beam is modelled by reducing stiffness of the selected elements. Reduction of stiffness is achieved by decreasing thickness of elements in the damaged region of the beam, which consequently reduces the moment of inertia I. The modal frequencies and corresponding mode shapes for the first 15 flexural modes of both the healthy and the damaged beams were calculated.

3.2 Experimental set-up

Modal frequencies of the test beams were measured by the POLYTEC PSV-400-B scanning laser vibrometer (SLV). General experiment set-up consists of the PSV-I-400 LR optical scanning head equipped with the highly sensitivity vibrometer sensor (OFV-505), OFV-5000 controller, PSV-E-400 junction box, the amplifier Bruel&Kjaer type 2732, and the computer system with data acquisition board and PSV Software (Figure 2). The system requires defining geometry of the object and set up scanning grid. To match the finite element model 126 equally spaced

scanning points have been taken to cover the *Beam 1* along its length and 151 scanning points were set for the *Beam 2*. The free-free (all edges free) boundary conditions have been simulated during experiment by hanging up the beam with two thin threads. In order to simulate the clamped-clamped (two ends fixed) boundary conditions experimentally, two vices have been used to fix ends of the beam (10 mm from both sides) with the clamped torque equal 20 Nm. The beam has then been excited by an input periodic chirp signal generated by the internal generator with a 1600Hz bandwidth through a piezoelectric actuator (PZT). The excitation with small piezoelectric discs works via the radial expansion of the disc causing a bending moment to the beam surface. As a result of this excitation the beam starts to vibrate within the frequency band of the input signal. After the measurement is performed in one point, the vibrometer automatically moves the laser beam to another point of the scan grid, measures the response using the Doppler principle and validates the measurement with the signal-to-noise ratio. The procedure is repeated until all scan points have been measured. The modal frequencies and corresponding mode shapes are obtained by taking the Fast Fourier Transform of the response signal.

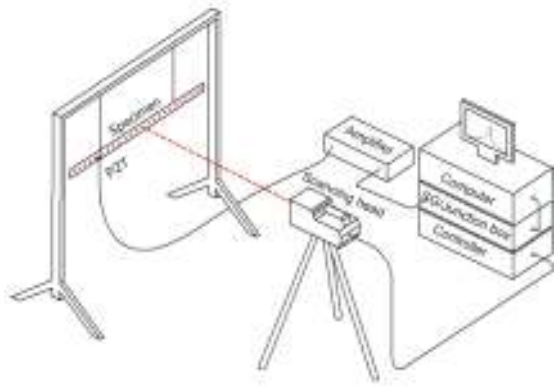

Fig.2. Scheme of experimental set-up.

3.3 Results of damage detection

Results of the mode shape based damage detection methods are given in Figures 3 and 4. For comparison purposes the damage indexes are also calculated employing the mode shape information obtained via the finite element simulations. From the results presented in Figure 3 MSC and MSCS damage index methods as well as the proposed MSCSM damage index method succeeded in pointing out the damage size and location. From the damage indexes obtained by using the numerically calculated mode shape information it is seen that the largest peak value appears at the location of the damage demonstrating that the proposed damage index methods can successfully detect and locate damage. When the experimentally measured mode shape information is employed large peak is observed at the location of the damage, however, the largest peaks appear at the boundaries of the beam. This could be explained by the free-free (FF) boundary conditions used in the experiment which results in maximum deflection at the boundaries and therefore subsequently leads to maximum measurement noise at the boundaries. In order to minimize the effect of the boundary conditions on mode shape information, it was decided to test the beams with the clamped-clamped (CL) boundary conditions. Again, two out of four methods included in the investigation for comparison purposes as well as the proposed MSCSM damage index method were capable of indicating the location and size of the damage. MSCS and MSCSM damage index plots for the beams with the CL boundary conditions are presented in Figure 4. One can see that this time the largest peaks in MSCSM damage index plot are seen at the location of the damage.

3.4 Identification of damage extent

Employing the proposed damage detection method the location and size of the damage was correctly found. Once the location and size of the damage was detected, the following interest was to identify damage extent or in this case the depth of damage. The extent of the damage was identified via modal frequencies by using a mixed numerical-experimental technique. The method is based on the minimization of the discrepancy between the numerically calculated and experimentally measured frequencies. For this the first 10 flexural frequencies of the beams with the free-free boundary conditions have been used. The free-free boundary conditions were selected because of the best correlation between the numerically calculated and experimentally measured modal frequencies. In Table 1 modal frequencies for the first 10 flexural modes for both, the healthy and damaged state of the beams with the free-free boundary conditions, have been listed. Residuals characterizing differences between experimental and numerical frequencies were calculated by the following expression

$$\Delta_i = \frac{\left|\omega_i^{FEM} - \omega_i^{EXP}\right|}{\omega_i^{EXP}} \times 100 \qquad (13)$$

where ω_i^{FEM} and ω_i^{EXP} are numerically calculated and experimentally measured modal frequencies, respectively and i denotes mode number. One can see that residuals between the numerical and experimental frequencies for the healthy beams are very small, which indicate that the finite element model has been constructed correctly. On the other hand, frequency residuals for the damaged beams are significantly larger, which indicates that the finite element model has some imperfections, for example, damage representation may not be correct. The damage depth in the beams has been modelled by reducing thickness (h_1 = 3mm) of the selected elements. Since the damage in the beams was introduced manually by means of a mill, the accuracy of the damage depth could be guaranteed only to the certain limit.

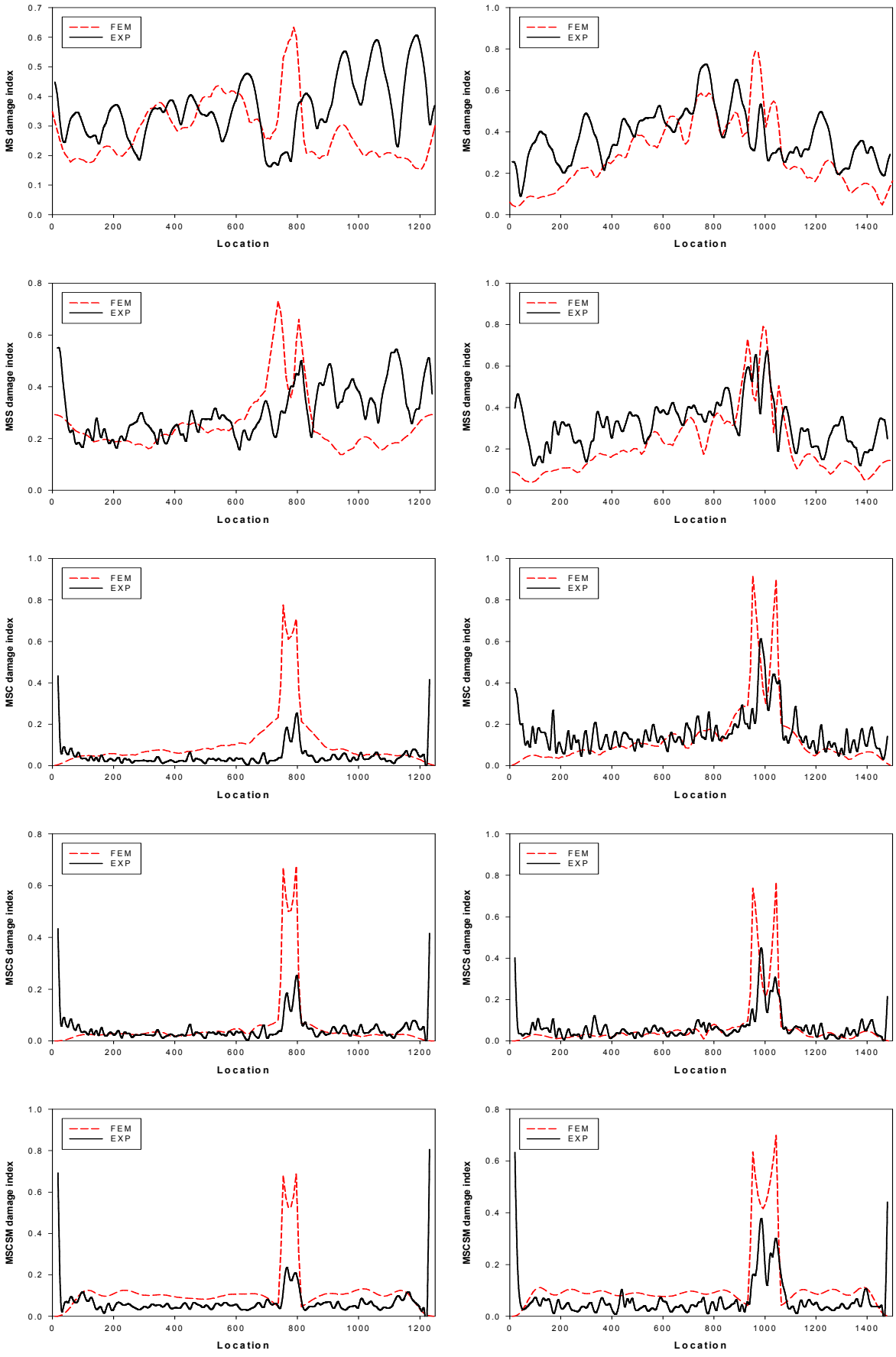

Figure 3 - Damage detection methods for beams with FF boundary conditions; *Beam1* – left; *Beam 2* – right.

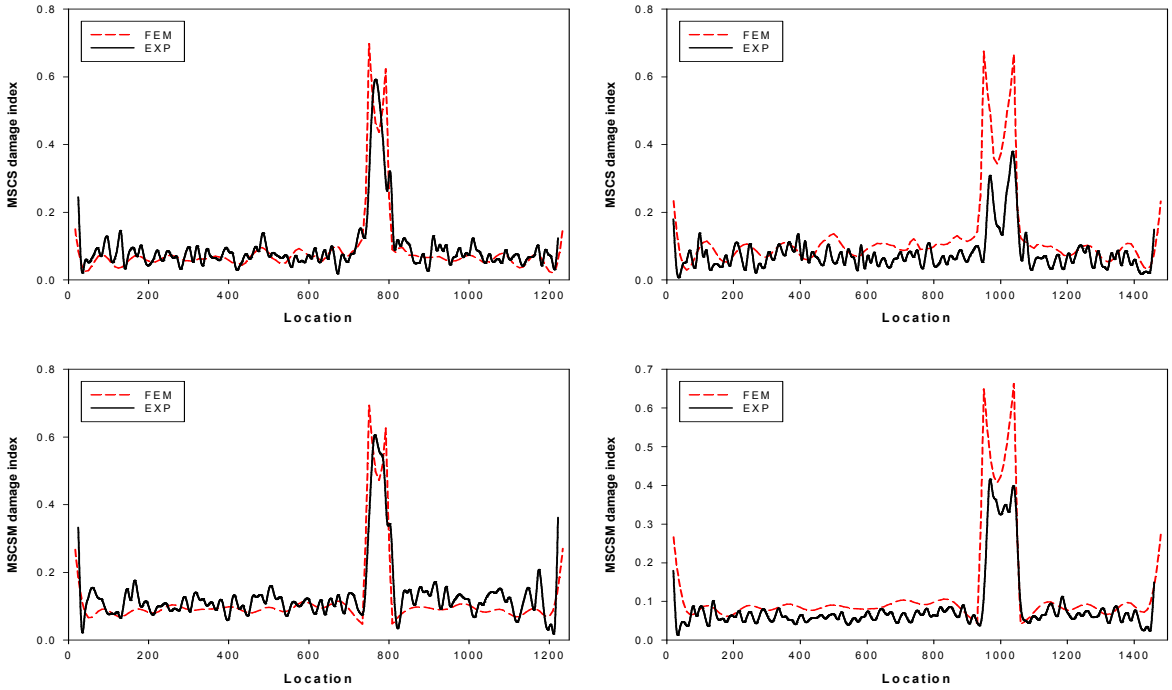

Figure 4 - Damage detection methods for beams with CL boundary conditions; *Beam1* – left; *Beam 2* – right.

Table 1 - Flexural frequencies and residuals for the *Beam 1* and the *Beam 2* with FF boundary conditions

Mode (i)	*Beam 1*						*Beam 2*					
	Healthy			Damaged			Healthy			Damaged		
	$\omega_{i\,EXP}^{h}$ (Hz)	$\omega_{i\,FEM}^{h}$ (Hz)	Δ_i (%)	$\omega_{i\,EXP}^{d}$ (Hz)	$\omega_{i\,FEM}^{d}$ (Hz)	Δ_i (%)	$\omega_{i\,EXP}^{h}$ (Hz)	$\omega_{i\,FEM}^{h}$ (Hz)	Δ_i (%)	$\omega_{i\,EXP}^{d}$ (Hz)	$\omega_{i\,FEM}^{d}$ (Hz)	Δ_i (%)
1	16.50	16.60	0.61	14.25	14.76	3.45	11.50	11.53	0.25	9.75	9.91	1.61
2	45.50	45.76	0.56	42.25	43.03	1.82	31.75	31.78	0.09	28.00	28.12	0.42
3	89.25	89.70	0.50	88.50	89.15	0.73	62.00	62.29	0.47	61.00	61.30	0.49
4	147.50	148.27	0.52	136.75	138.78	1.46	102.50	102.97	0.46	97.75	98.15	0.41
5	220.50	221.47	0.44	216.25	217.82	0.72	153.25	153.81	0.37	144.50	145.01	0.35
6	308.00	309.30	0.42	299.00	301.15	0.71	214.00	214.82	0.38	206.25	208.77	1.21
7	409.50	411.75	0.55	391.00	394.98	1.01	284.75	285.98	0.43	272.25	274.53	0.83
8	526.50	528.80	0.44	519.25	523.01	0.72	366.00	367.29	0.35	351.75	353.14	0.39
9	659.00	660.46	0.22	635.00	638.42	0.54	457.75	458.75	0.22	433.00	438.24	1.20
10	806.25	806.71	0.06	784.25	787.38	0.40	559.50	560.36	0.15	537.50	539.47	0.36
Aver.			0.43			1.16			0.32			0.73

It is assumed that the damage size and location have been set correctly and thus thickness h_1 of the damage elements is selected as the parameter to be identified. The domain of interest for thickness h_1 was selected as follows

$$2.7 \le h_1 \le 3.3\,\text{mm} \qquad (14)$$

Accuracy step of 0.1mm was selected and the finite element calculations in this domain were performed. Then employing the response surface approach the obtained data were used to build the approximating functions (second order polynomial functions) for all 10 flexural frequencies. These approximating functions represent the relationship between the modal frequencies ω_i and thickness h_1 of the damage elements. For the identification of thickness two identification functionals were proposed. The first one uses modal frequencies from both, the healthy and the damaged states of the beam and is defined by

$$\Phi_1(h_1) = \sum_{i=1}^{I} \left[\frac{\left(\omega_{i\,FEM}^{h} \dfrac{\omega_{i\,EXP}^{d}}{\omega_{i\,EXP}^{h}} \right)^2 - \left(\omega_{i\,FEM}^{d}(h_1) \right)^2}{\left(\omega_{i\,FEM}^{h} \dfrac{\omega_{i\,EXP}^{d}}{\omega_{i\,EXP}^{u}} \right)^2} \right]^2 ; \quad (15)$$

$$i = 1,2,...,I$$

where $\omega_{i\,EXP}^{h}$ and $\omega_{i\,EXP}^{d}$ are the experimentally measured modal frequencies of the healthy and the damaged states of the beams, respectively, $\omega_{i\,FEM}^{h}$ are

numerically calculated modal frequencies of the healthy state of the beams and $\omega_{i\,FEM}^{d}(h_1)$ are approximating functions representing the relationship between the modal frequencies and thickness of the damage elements. I is the number of frequencies used in the functional. The idea of this functional is based on the assumption that the numerical frequency ratio $\omega_{i\,FEM}^{h} / \omega_{i\,FEM}^{d}$ should be close to the experimental one $\omega_{i\,EXP}^{h} / \omega_{i\,EXP}^{d}$.

The second proposed identification functional uses modal frequencies only from the damaged state of the beam and is given as

$$\Phi_2(h_1) = \sum_{i=1}^{I} \left(\frac{\omega_{i\,EXP}^{d\ 2} - \omega_{i\,FEM}^{d}(h_1)^2}{\omega_{i\,EXP}^{d\ 2}} \right)^2; \qquad (16)$$

$$i = 1,2,...,I$$

The damage extent is obtained by minimizing the identification functional $\Phi(h_1)$ subjected to the lower $h_1^{\min}$ and upper $h_1^{\max}$ bounds of the identification parameter. Minimizing the first identification functional (15), the following thickness of the damage elements were obtained: for the *Beam 1* - h_1 = 2.81 mm, for the *Beam 2* - h_1 = 2.93 mm. Employing the second functional (16): for the *Beam 1* - h_1 = 2.76 mm, for the *Beam 2* - h_1 = 2.89 mm. Now, when the thickness of the damage elements was obtained, it was of interest to evaluate the accuracy of the identification. Verification of the obtained results was performed by numerically calculating modal frequencies in the point of optimum (using the identified thickness of the damage elements).

Table 2 - Flexural frequencies and residuals for the *Beam 1* calculated using identified damage extent.

Mode (i)	*Beam 1*						
		h_1=3 mm		h_1=2.81 mm		h_1=2.76 mm	
	$\omega_{i\,EXP}^{d}$ (Hz)	$\omega_{i\,FEM}^{d}(h_1)$ (Hz)	Δ_i (%)	$\omega_{i\,FEM}^{d}(h_1)$ (Hz)	Δ_i (%)	$\omega_{i\,FEM}^{d}(h_1)$ (Hz)	Δ_i (%)
1	14.25	14.76	3.45	14.33	0.58	14.21	0.30
2	42.25	43.03	1.82	42.52	0.64	42.38	0.31
3	88.50	89.15	0.73	89.02	0.59	88.99	0.55
4	136.75	138.78	1.46	137.29	0.39	136.88	0.10
5	216.25	217.82	0.72	217.21	0.44	217.04	0.36
6	299.00	301.15	0.71	299.87	0.29	299.52	0.17
7	391.00	394.98	1.01	393.11	0.54	392.63	0.42
8	519.25	523.01	0.72	521.32	0.40	520.79	0.30
9	635.00	638.42	0.54	636.16	0.18	635.58	0.09
10	784.25	787.38	0.40	784.57	0.04	783.76	0.06
Aver.			1.16		0.41		0.27

Table 3 - Flexural frequencies and residuals for the *Beam 2* calculated using identified damage extent.

Mode (i)	*Beam 2*						
		h_1=3 mm		h_1=2.93 mm		h_1=2.89 mm	
	$\omega_{i\,EXP}^{d}$ (Hz)	$\omega_{i\,FEM}^{d}(h_1)$ (Hz)	Δ_i (%)	$\omega_{i\,FEM}^{d}(h_1)$ (Hz)	Δ_i (%)	$\omega_{i\,FEM}^{d}(h_1)$ (Hz)	Δ_i (%)
1	9.75	9.91	1.61	9.79	0.36	9.71	0.40
2	28.00	28.12	0.42	27.92	0.29	27.81	0.70
3	61.00	61.30	0.49	61.23	0.37	61.18	0.30
4	97.75	98.15	0.41	97.90	0.16	97.76	0.01
5	144.50	145.01	0.35	144.69	0.13	144.52	0.01
6	206.25	208.77	1.21	208.24	0.96	207.91	0.80
7	272.25	274.53	0.83	273.95	0.62	273.62	0.50
8	351.75	353.14	0.39	352.72	0.27	352.48	0.21
9	433.00	438.24	1.20	436.54	0.81	435.52	0.58
10	537.50	539.47	0.36	538.48	0.18	537.92	0.08
Aver.			0.73		0.42		0.36

According to the results given in Tables 2 and 3, the average frequency residuals for the damaged beams are considerably smaller compared to the average residuals when nominal thickness of the damage elements is employed. The residuals for the damaged beams do not exceed 1% and a good agreement between the average frequency residuals of the healthy and the damaged beams is observed. From this it can be concluded that both identification functionals were capable to identify the damage extent. Second one showing slightly better results (the average residuals for the damaged beams are smaller). It suggests that the damage location, size and extent in the beam structure can be obtained without prior knowledge of the healthy state of structure.

4. Case study 2 – aluminium beams with multiple damage locations

To elaborate the proposed damage detection method two aluminium beams containing multiple mill-cut damage locations are examined.

4.1 Geometry of the beams and numerical analysis

Geometrical configuration of the beams is shown in Figure 5. Dimensions of the *Beam 3* are as follows: length L = 1250 mm, width B = 50 mm and thickness H = 5 mm. Mill-cut damage with depth of 2 mm and size of 50 mm is introduced at two locations of the beam with a distance of 450 mm from both edges of the beam. The *Beam 2* dimensions are 1500 x 50 x 5 mm. Damage with depth of 2 mm and size of 100 mm is also introduced at two locations of the beam with a distance of 450 mm from both edges of the beam.

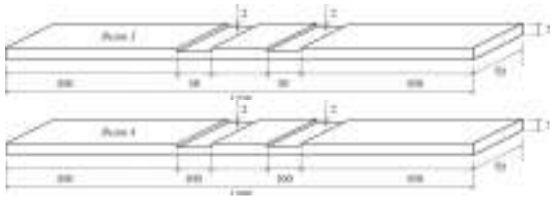

Fig.5. Geometry and dimensions of the test beams containing mill-cut damage at multiple locations.

Material properties are selected the same as for the beams with a single damage location. Finite element length of 10 mm is considered, thus the *Beam 3* is constructed by means of 125 equal length elements (i=126 nodes) and the *Beam 4* -150 elements (i=151 nodes). The damage in beams is modelled in the same way as for the beams with a single damage location. Again, the modal frequencies and corresponding mode shapes for the first 15 flexural modes of both the healthy and the damaged beams were numerically calculated and experimentally measured.

4.2 Results of damage detection

For the beams with multiple damage locations only the clamped-clamped (CL) boundary conditions were considered. Results for MSCS and MSCSM damage index are given in Figure 6. For comparison purposes the damage indexes were also calculated employing the mode shape information obtained via the finite element simulations. One can see that both damage index methods were capable of pointing out the damage size and location.

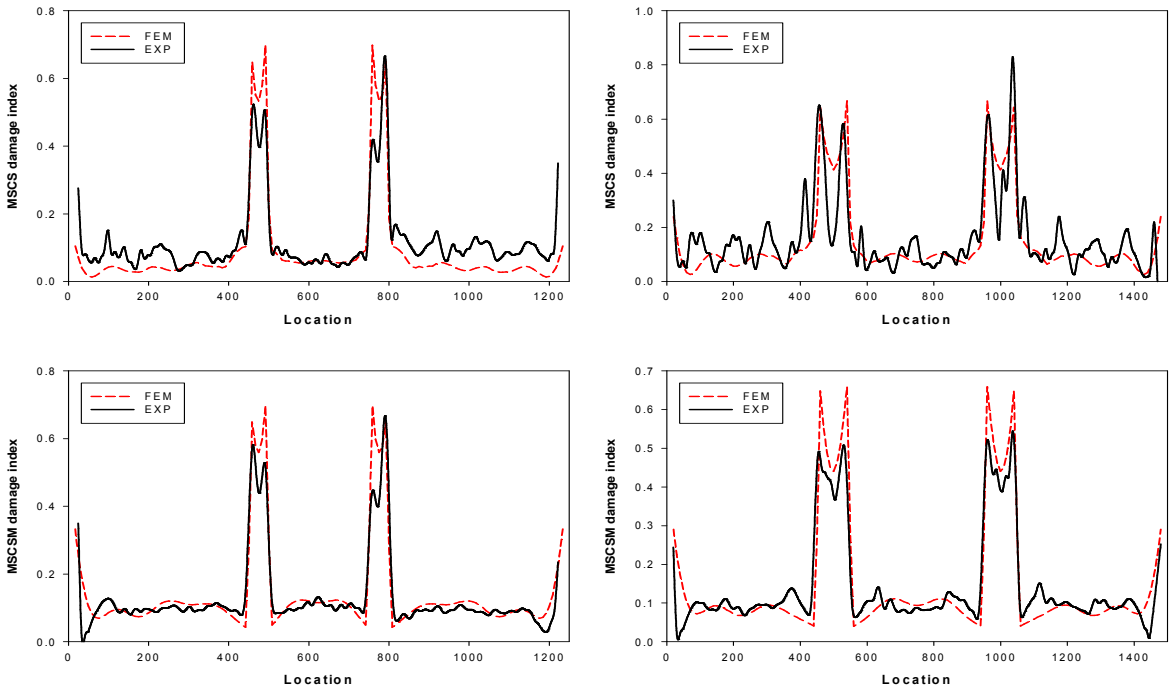

Fig.6. Damage detection methods for beams with multiple damage locations; *Beam 3* – left; *Beam 4* – right.

4.3 Identification of damage extent

Employing the proposed damage detection method both damage locations was successfully pointed out. Again, the following interest was to identify damage extent. The extent of the damage was identified by using the same procedure described in section 3.4. In Table 4 modal frequencies for the first 10 flexural modes of the beams with the free-free boundary conditions, have been presented. As it can be seen frequency residuals for the damaged beams again are significantly larger than for the healthy beams, which suggest that damage representation in the finite element simulations has to be improved. Since it is assumed that the damage size and location have been set correctly then the damage depth is selected as the parameter to be identified. Initially the damage depth in the beams has been modelled by reducing thickness (h_1 = 3mm) of the selected elements equally at both damage locations. In the process of identification reduced thickness of the damaged elements at both damage locations was assumed to be equal and thus the domain of interest for thickness was selected as follows

$$2.7 \le h_1 \le 3.3 \text{ mm} \tag{14}$$

Minimizing the first identification functional (15), the following results were obtained: for the *Beam 3* - h_1 = 2.94 mm, for the *Beam 4* - h_1 = 2.95 mm. Employing the second functional (16): for the *Beam 3* - h_1 = 2.90 mm, for the *Beam 4* - h_1 = 2.93 mm. Verification of the obtained results is presented in Tables 5and 6.
One can see from the presented results that now the average frequency residuals for the damaged beams are considerably smaller compared to the average residuals when nominal thickness of the damage elements is employed.

Table 4 - Flexural frequencies and residuals for the *Beam 3* and the *Beam 4* with FF boundary conditions

Mode (i)	*Beam 3*						*Beam 4*					
	Healthy			Damaged			Healthy			Damaged		
	$\omega_{i\,EXP}^{h}$ (Hz)	$\omega_{i\,FEM}^{h}$ (Hz)	Δ_i (%)	$\omega_{i\,EXP}^{d}$ (Hz)	$\omega_{i\,FEM}^{d}$ (Hz)	Δ_i (%)	$\omega_{i\,EXP}^{h}$ (Hz)	$\omega_{i\,FEM}^{h}$ (Hz)	Δ_i (%)	$\omega_{i\,EXP}^{d}$ (Hz)	$\omega_{i\,FEM}^{d}$ (Hz)	Δ_i (%)
1	16.50	16.60	0.61	13.49	13.25	1.75	11.50	11.53	0.25	8.90	8.75	1.74
2	45.50	45.76	0.56	39.42	38.75	1.71	31.75	31.78	0.09	23.86	23.50	1.52
3	89.25	89.70	0.50	88.70	88.25	0.51	62.00	62.29	0.47	60.17	59.75	0.69
4	147.50	148.27	0.52	130.36	128.75	1.24	102.50	102.97	0.46	94.71	94.00	0.75
5	220.50	221.47	0.44	213.14	210.75	1.12	153.25	153.81	0.37	135.53	134.50	0.76
6	308.00	309.30	0.42	295.56	294.00	0.53	214.00	214.82	0.38	202.69	201.25	0.71
7	409.50	411.75	0.55	375.80	371.75	1.08	284.75	285.98	0.43	264.75	262.75	0.76
8	526.50	528.80	0.44	517.16	513.00	0.80	366.00	367.29	0.35	339.24	338.00	0.37
9	659.00	660.46	0.22	621.34	618.00	0.54	457.75	458.75	0.22	420.72	418.25	0.59
10	806.25	806.71	0.06	764.13	759.25	0.64	559.50	560.36	0.15	515.45	512.50	0.57
Aver.			0.43			0.99			0.32			0.85

Table 5 - Flexural frequencies and residuals for the *Beam 3* calculated using identified damage extent.

Mode (i)	*Beam 3*						
		h_1=3 mm		h_1=2.94 mm		h_1=2.90 mm	
	$\omega_{i\,EXP}^{d}$ (Hz)	$\omega_{i\,FEM}^{d}(h_1)$ (Hz)	Δ_i (%)	$\omega_{i\,FEM}^{d}(h_1)$ (Hz)	Δ_i (%)	$\omega_{i\,FEM}^{d}(h_1)$ (Hz)	Δ_i (%)
1	13.49	13.25	1.75	13.30	0.40	13.18	0.55
2	39.42	38.75	1.71	39.00	0.65	38.71	0.10
3	88.70	88.25	0.51	88.64	0.44	88.60	0.39
4	130.36	128.75	1.24	129.54	0.61	128.99	0.18
5	213.14	210.75	1.12	212.67	0.90	212.35	0.75
6	295.56	294.00	0.53	294.97	0.33	294.57	0.19
7	375.80	371.75	1.08	374.46	0.72	373.57	0.49
8	517.16	513.00	0.80	516.19	0.62	515.50	0.49
9	621.34	618.00	0.54	620.07	0.33	619.22	0.20
10	764.13	759.25	0.64	762.41	0.41	761.25	0.26
Aver.			0.99		0.54		0.36

Table 6 - Flexural frequencies and residuals for the *Beam 4* calculated using identified damage extent.

Mode (i)	*Beam 4*						
		h_1=3 mm		h_1=2.95 mm		h_1=2.93 mm	
	$\omega_{i\,EXP}^{d}$ (Hz)	$\omega_{i\,FEM}^{d}(h_1)$ (Hz)	Δ_i (%)	$\omega_{i\,FEM}^{d}(h_1)$ (Hz)	Δ_i (%)	$\omega_{i\,FEM}^{d}(h_1)$ (Hz)	Δ_i (%)
1	8.90	8.75	1.74	8.79	0.43	8.74	0.11
2	23.86	23.50	1.52	23.52	0.10	23.39	0.49
3	60.17	59.75	0.69	60.05	0.51	60.01	0.43
4	94.71	94.00	0.75	94.43	0.46	94.32	0.34
5	135.53	134.50	0.76	135.06	0.41	134.87	0.27
6	202.69	201.25	0.71	201.98	0.36	201.69	0.22
7	264.75	262.75	0.76	263.91	0.44	263.57	0.31
8	339.24	338.00	0.37	338.76	0.22	338.57	0.17
9	420.72	418.25	0.59	418.76	0.12	417.96	0.07
10	515.45	512.50	0.57	513.45	0.18	512.62	0.02
Aver.			0.85		0.32		0.24

5. Conclusions

The present study focuses on the identification of a mill-cut damage location, size and extent in a beam structure by extracting dynamic characteristics obtained from vibration experiments. It was proposed to use the magnitude of the mode shape curvature square for the detection of the damage location and size. Compared to the existing damage detection methods such as MSC and MSCS damage index methods, the advantage of the proposed method is that it requires mode shape information only from the damaged state of the structure and can give reliable results in more simple way. In order to reduce the influence of measurement noise on the damage detection from the experimentally measured mode shape information it was proposed to use the average sum of the mode shape curvature squares for all modes. Effectiveness and robustness of the present method is demonstrated by two aluminium beams containing mill-cut damage at single location as well as for two aluminium beams with damage at multiple locations. It can be concluded that the clamped-clamped instead of the free-free boundary conditions for the beam structure is recommended for the detection of the damage location and size. The extent of mill-cut damage has been identified via modal frequencies by using a mixed numerical-experimental technique. The proposed method is based on the minimization of the discrepancy between the numerically calculated and experimentally measured frequencies. Obtained results showed that thickness of the beam in damage region differs from the originally set nominal value, which is explained by the fact that the mill cut damage in the beams was introduced manually by means of a mill.

Acknowledgements

This work was partially supported by the European Commission under Framework Program 6, project MOMENTUM, Contract No. MRTN-CT-2005-019198.

References

1. **Hall, S.R. and Conquest, T.J.** "The Total Data Integrity Initiative - Structural Health Monitoring, The Next Generation", Proceedings of the USAF ASIP conference. 2nd edition, 1999.
2. **Doebling, S.W., Farrar, C.R., Prime, M.B. and Shevitz, D.W.** "Damage Identification and Health Monitoring of Structural and Mechanical Systems From Changes in Their Vibration Characteristics: A Literature Review", Los Alamos National Laboratory Report LA-13070-MS, 1996.
3. **Xia, Y.** "Condition Assessment of Structures Using Dynamic Data", PhD. thesis, Nanyang Technology University, Singapore, 2002.
4. **Ho, Y.K. and Ewins, D.J.** "On structural damage identification with mode shapes", Proceedings of COST F3 Conference on System Identification and Structural Health Monitoring, Madrid, Spain, pp. 677–686, 2000,.
5. **Stubbs, N. and Kim, J.T.** "Damage Localization in Structures without Baseline Modal Parameters", American Institute of Aeronautics and Astronautics Journal, 34(8), pp. 1649–1654, 1996.
6. **Yuen, M.M.F.** "A Numerical Study of the Eigenparameters of a Damaged Cantilever", Journal of Sound and Vibration, 103, pp. 301–310, 1985.
7. **Pandey, A.K., Biswas, M. and Samman, M.M.** "Damage Detection from Changes in Curvature Mode Shapes", Journal of Sound and Vibration, 145(2), pp. 321–332, 1991.
8. **Wahab, A. and Roeck, G.** "Damage Detection in Bridges Using Modal Curvatures: Application to a Real Damage Scenario", Journal of Sound and Vibration, 226, 217–235, 1999.
9. **Maia, N.M.M, Silva, J.M.M., Almas, E.A.M and Sampaio R.P.C.** "Damage Detection in

Structures: from Mode Shape to Frequency Response Function Methods", Mechanical Systems and Signal Processing, 17(3), pp. 489-498, 2003.

10. **Wu, D. and Law S.S.** "Damage Localization in Plate Structures from Uniform Load Surface Curvature", Journal of Sound and Vibration, 276, pp. 227–244, 2004.
11. **Ratcliffe, C.P. and Bagaria, W.J.** "A Vibration Technique for Locating Delamination in a Composite Beam", American Institute of Aeronautics and Astronautics Journal, 36(6), pp. 1074–1077, 1998.
12. **Gherlone, M., Mattone, M., Surace, C., Tassoti, A., Tessler, A.** "Novel Vibration-Based Methods for Detecting Delamination Damage in Composite Plate and Shell Laminates", Key Engineering Materials, 293-294, pp. 289-296, 2005.